High Fidelity Failure Analysis for A Composite Fuselage Section

Jian Li
Engineer/Scientist, The Boeing Company
Mesa, Arizona
Jian.Li@Boeing.com

Carlos G. Dávila
Aerospace Engineer, NASA Langley Research Center
Hampton, Virginia
C.G.Davila@Larc.NASA.Gov

Tzi-Kang Chen
Research Engineer, Army Research Laboratory
Hampton, Virginia
T.Chen@Larc.NASA.Gov

ABSTRACT

A high fidelity delamination failure analysis was developed by combining a local failure analysis with a global full-scale finite element structural analysis to address strength and delamination failure in a single package. The methodology was demonstrated through a local three-dimensional pull-off failure analysis and a geometrically nonlinear structural analysis of a five-foot composite helicopter fuselage section. Pull-off specimens were used to identify potential debonding failure of co-cured skin-stringer/frame fuselage structures. An investigation of the failed pull-off specimens was performed to determine the location of the failure initiation. Three-dimensional strain energy release rate analysis indicates that the delamination initiation and growth is controlled by Mode I opening mode. The bending moment at the delamination tip was identified as the crucial factor controlling the failure. The geometrically nonlinear structural analysis of a five-foot composite fuselage section was performed using a detailed finite element model. Loads were applied along the periphery of the subcomponent using displacement fields generated from solutions of a full-vehicle model.

INTRODUCTION

Before advanced composites can be used in primary structures of the next generation of helicopters, significant technological advancements will have to be realized to reduce the cost of the traditional building block approach to composite structure certification [1]. The colossal amount of testing required for structural flight certification can only be reduced by incorporating more accurate and more efficient analyses into the earliest phases of the design. It is well known that because of the weakness of composites in the transverse direction and the complexity of their failure modes, the analysis of composite structures requires a higher degree of fidelity than their metallic counterparts.

A high fidelity analysis methodology is proposed to address the limited accuracy and high computational cost of current strength analyses. The methodology is based on a delamination failure analysis of composite skin-frame/stringer pull-off test specimens and a global non-linear shell finite element analysis (FEA) of the entire structure. A delamination failure analysis of the pull-off specimen was performed. The critical bending moment at the delamination tip was identified as the dominant factor contributing to failure. A global finite element analysis was used to compute the out-of-plane bending moments along with strains throughout the entire structure. In addition to comparing the strains against the strain allowable, the out-of-plane bending moments were checked against the delamination failure allowable established from pull-off tests.

The present methodology identifies potential failures early during the analysis stage, rather than at the end of a full-scale structural test. The analysis methodology is easy to use because the current finite element analysis computes the out-of-plane bending moments explicitly, and these can easily be used to compute the margins of safety in delamination. The allowable bending moment is readily established from pull-off and other limited fracture toughness coupon tests. The methodology is applicable to any integrally stiffened composite skin-frame/stiffener structures, with wide ranging applications in the aerospace industry.

LOCAL FAILURE ANALYSIS

Pull-off Failure

Pull-off tests are useful in identifying the failure mode between the composite skin and the frame in co-cured

Presented at the American Helicopter Society 57th Annual Forum, Washington, DC, May 9-11, 2001.

composite skin-stringer/frame fuselages. A schematic of a pull-off specimen and its failure mode is shown in Fig. 1. The pre-cured frame was inserted into the angle clip preform on the skin preform and then vacuum bagged and co-cured with the angle clip and the skin preforms. The pull-off specimens consist of 2.5-in.-wide sections cut from the cured frame and skin panel. The pull-off tests were conducted by pulling the frame while fixing down both ends of the skin. The free span L shown in Fig. 1 denotes the distance between the fixed ends. The failure modes observed in the pull-off tests were dominated by delamination between the skin and the angle clip starting from a crack in the resin-rich corner.

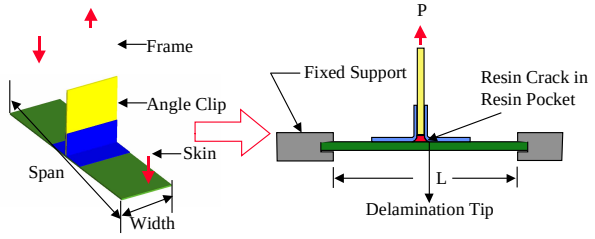

Fig. 1. Schematic of the pull-off specimen and failure location.

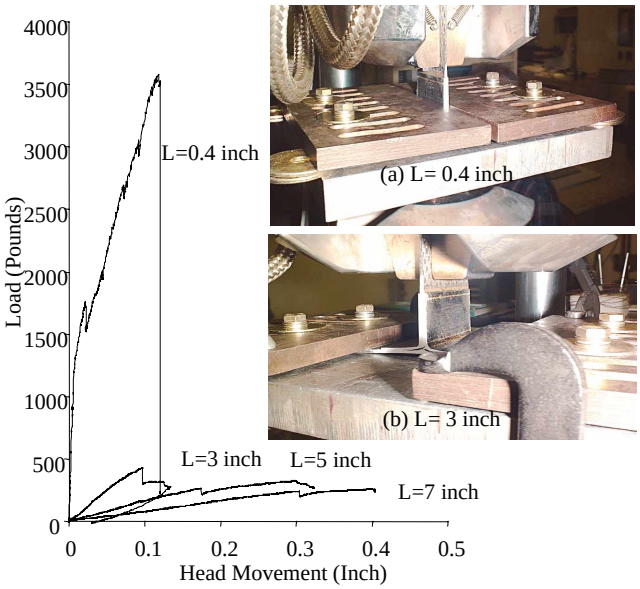

Fig. 2. Effect of the free span on the pull-off load.

Four pull-off specimens were tested at four different spans of 7, 5, 3 and 0.4 (at the root) inches. The span (L) effect on the pull-off load is shown in Figure 2. As the span L decreases, the pull-off load increases. The failure mode is delamination between the angle clip and the skin initiating at the corner as seen from the inserted photo in Fig. 2b. Even when the support clamps are placed next to the frame (Fig. 2a) to clamp down the angle clip and skin separation, no shear failure was observed between the frame and the angle clip.

Delamination Failure Criterion

As observed from the pull-off tests, the pull-off failure mode is dominated by delamination between the skin and the angle clip starting from a resin crack at the corner. The best way to study the crack-delamination failure is to place a defect right at this critical location and investigate the defect initiation and growth under a pull-off load. The strain energy release rate approach has been applied effectively to the analysis of the delamination failure in composite hat stringer pull-off specimens [2-4]. The strain energy release rate is the measure of the loss of strain energy as new delamination surface area is created.

Delaminations are typically mixed-mode fracture phenomena consisting of a combination of an opening Mode I due to interlaminar tension, a sliding shear Mode II due to interlaminar shear, and a scissoring shear Mode III due to anti-plane shear. The total strain energy release rate, G_T, consists of contributions due to opening mode fracture, G_I, sliding shear fracture, G_{II}, and scissoring shear fracture, G_{III}. Hence, $G_T=G_I+G_{II}+G_{III}$. Test methods have been proposed in the past to characterize fracture toughness in each of the three delamination modes [5]. For the two-dimensional pull-off specimen analysis [2-3], $G_{III}=0$, $G_T=G_I+G_{II}$ and the delamination initiation is governed by G_I and G_{II}.

In Ref. 2, the mixed mode fracture toughness, G_c, was presented as a function of the mixed mode ratio G_{II}/G_T for carbon/toughened epoxy unidirectional prepreg composites. Delamination initiates when the applied G_T reaches the material fracture toughness (G_c) at the applied mixed mode ratio as

$$G_T\left(G_{II}/G_T\right)=G_c\left(G_{II}/G_T\right) \qquad (1)$$

For three-dimensional strain energy release rate analyses of the pull-off specimens, all three components of the strain energy release rate can coexist. To predict failure, the two-dimensional failure curves expressed in the right hand side of Eq. 1 should be expanded to a three-dimensional failure surface. However, generating a failure surface requires a great number of fracture toughness tests such as mixed mode I and mode III and mixed mode II and mode III, both of which are not available as mature test methods. To avoid these difficulties, Ref. 4 proposed a shearing mode concept to combine the shearing modes to take advantage of the two-dimensional fracture toughness curve. For three-dimensional analysis, Eq. 1 takes the following form

$$G_T\left[\left(G_{shear}\right)/G_T\right]=G_c\left[\left(G_{shear}\right)/G_T\right] \qquad (2)$$

where $$G_{shear}=G_{II}+G_{III} \qquad (3)$$

This hypothesis needs experimental verification. For cases where the modes peak at different locations, Eq. 2 is equivalent to Eq. 1 and no accuracy is lost if the hypothesis turns out to be inaccurate for fully mixed cases.

Three-Dimensional Analysis

A three-dimensional finite element model was created to calculate the strain energy release rate along the defect. Due to symmetry, a quarter of the pull-off specimen was modeled with three-dimensional solid elements, as shown in Fig. 3. The finite element mesh consists of 8-noded brick elements with a total of 45696 elements in the model shown in Fig. 3. The virtual crack closure technique (VCCT) [6,7] was used to calculate the strain energy release rate components. A through-the-width crack of 0.08 inches was assumed at the delamination initiation front.

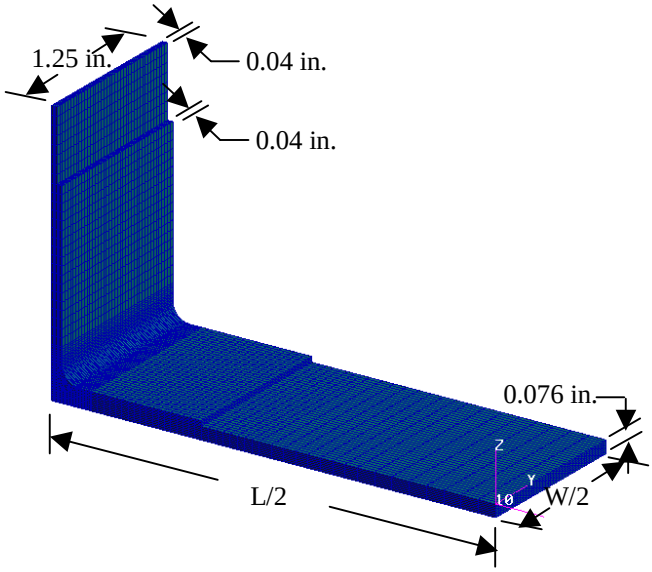

Fig. 3. Finite element model of 1/4 pull-off specimen.

The pull-off model shown in Fig. 3 was constructed from AS4 Plain Weave (PW) and 5-Harness satin (5H) fabric plies. The skin, frame and clip lay-ups were $[45^{5H}/0^{PW}/45^{5H}/0^{5H}]_s$, $[45^{5H}/0^{5H}/45^{5H}/0^{5H}]_s$ and $[45^{5H}/45^{5H}]_s$, respectively. The properties of the plain weave and 5-harness laminates used in the analysis are given in Table 1.

Table 1. FEM model material properties.

	Material		
Property	PW	5H	Unit
E_{xx}	10.2	10.2	Msi
E_{yy}	10.2	10.2	Msi
G_{xy}	0.55	0.55	Msi
ν_{xy}	0.05	0.05	
Ply thickness	0.008	0.01	inch

The strain energy release rate distribution along half the specimen width is shown in Fig. 4 under a pull-off load of 243 lb. In the interior region along the delamination front, the strain energy release rate is dominated by Mode I with a small Mode II contribution and no Mode III. The Mode I component drops dramatically near the edges of the defect while Mode II and Mode III components dominate in these regions. Laminated composites are much weaker against Mode I than mixed mode or Mode II. Thus, the delamination will initiate and grow from the center of the specimen by interlaminar tension. It is possible that after some initial growth, the delamination will be held at the edges until more energy is applied to grow the delamination further.

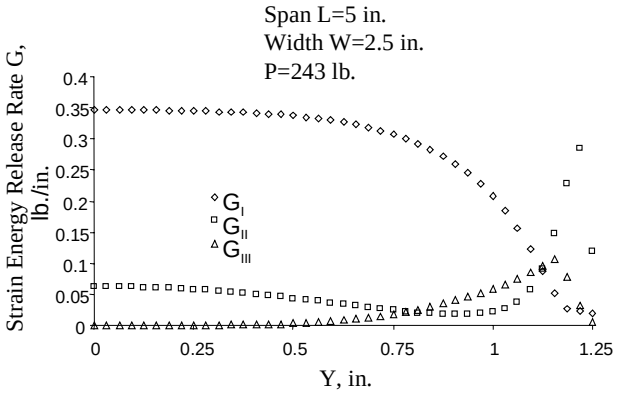

Fig. 4. Strain energy release rate distribution through half the width (from the center to the edge).

The mode mixity ratios in terms of Mode II, Mode III and the shearing mode are shown in Fig. 5. From the centerline to 0.5 inch of the width, the shearing mode ratio coincides with the Mode II ratio, while the Mode III ratio is almost zero in this region. The shearing mode ratio is used to predict delamination initiation and growth.

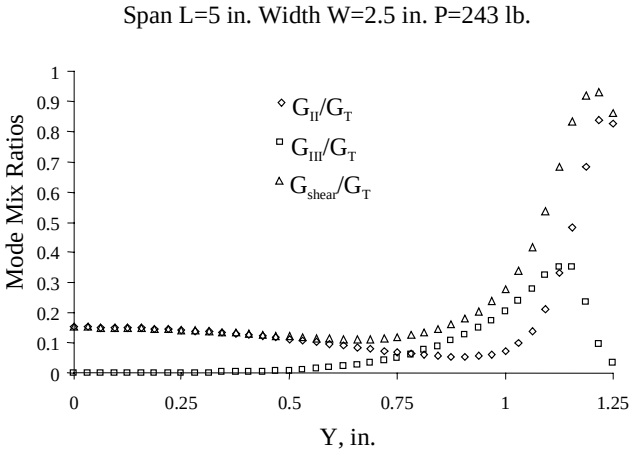

Fig. 5. Mode mixity distribution through half the width.

To predict the initiation and growth of the delamination from this defect, a mixed mode delamination criterion for the right hand side of Eq. 2 is required. Using the fracture toughness data given in Ref. 8 for AS4/3501-6 (Fig. 5), a mixed mode delamination criterion is obtained by fitting the data shown in Fig. 6.

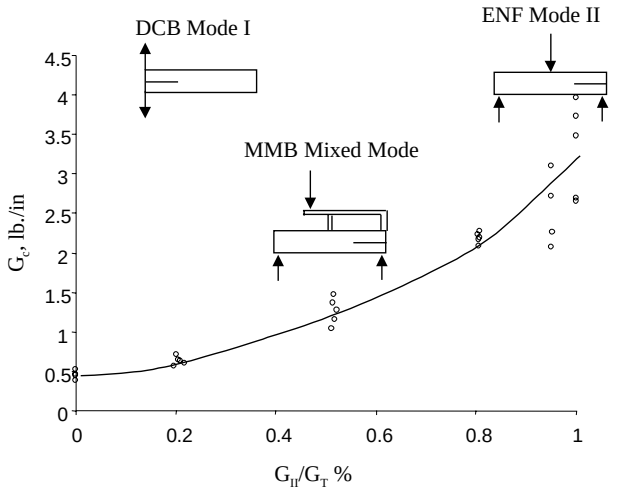

Figure 6. Fracture toughness data for AS4/3501-6 [8].

Using the hypothesis of Eq. 3, the mixed-mode criterion that fits the data in Figure 6 is

$$G_c = 0.43 + 1.23\left(\frac{G_{shear}}{G_T}\right) - 0.4\left(\frac{G_{shear}}{G_T}\right)^2 + 1.87\left(\frac{G_{shear}}{G_T}\right)^3 \qquad (4)$$

The critical pull-off load distribution through the width along the defect is calculated from

$$P_c = \sqrt{\frac{G_c}{G_T}}P/W \qquad (5)$$

where P_c is in lb./in.

The predicted critical pull-off load distributions along the defect through half the specimen width are shown in Fig. 7 for three different support spans. Three-dimensional predictions indicate a nearly constant pull-off load through most of the interior width of the specimen. Delamination initiates from the interior along the length of the specimen and then grows towards the edges. The predicted pull-off load decreases with the increase of the span. The critical pull-off load does not reach a plateau as the span increases. Thus, it is not possible to define the joint strength in terms of pull-off load.

On the other hand, the critical bending moment at the delamination front is nearly identical for all three support spans, as shown in Figure 8. Hence, the bending moment at the corner is proposed as a measure of the joint strength.

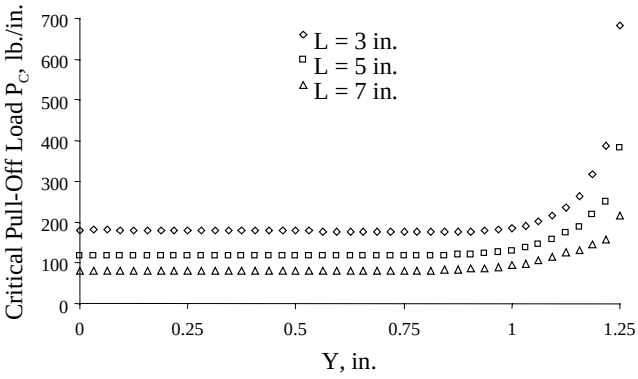

Fig. 7. Critical pull-off loads through half the width.

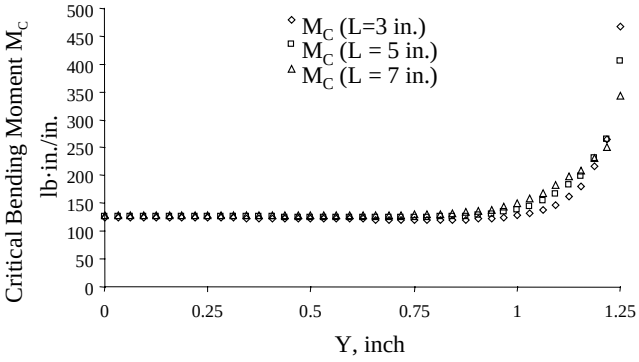

Fig. 8. Critical bending moment through half the width.

The use of the critical bending moment as a delamination failure criterion represents a significant step towards understanding the pull-off failure mechanism and easing the integration of the local and the global analyses. The local model no longer needs to be physically integrated into the global model of the actual structure since the global analysis already computes explicitly the out-of-plane bending moment throughout the structure.

GLOBAL ANALYSIS

The methodology described in the previous section was demonstrated through the analysis of the five-foot section of a composite fuselage shown in Fig. 9. The five-foot section was similar to the RWSTD (Rotary Wing

Structures Technology Demonstration) center fuselage [1] from frame stations (FM) 115 to 176. There are five frames and thirteen stringers in the model. The skin, stiffeners and frames from FS 115 to FS 176 were modeled by shell elements.

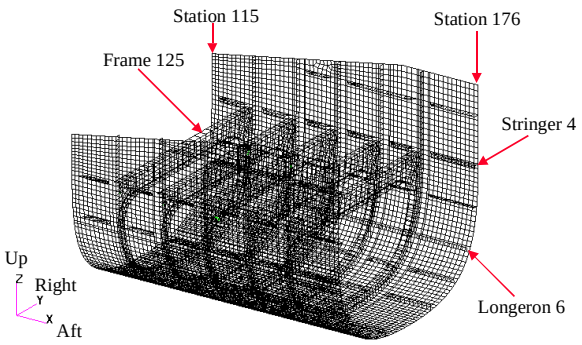

Fig. 9. Finite element model of the five foot sub-component.

The skin, stiffeners and frame lay-ups were the outcome of a traditional design approach that performs sizing using strength and buckling considerations. The displacements along the edges of the model were obtained from the solutions of a full helicopter finite element loads model. This loads model, which is shown in Fig. 10, has much less mesh refinement than the subcomponent model shown in Fig. 9.

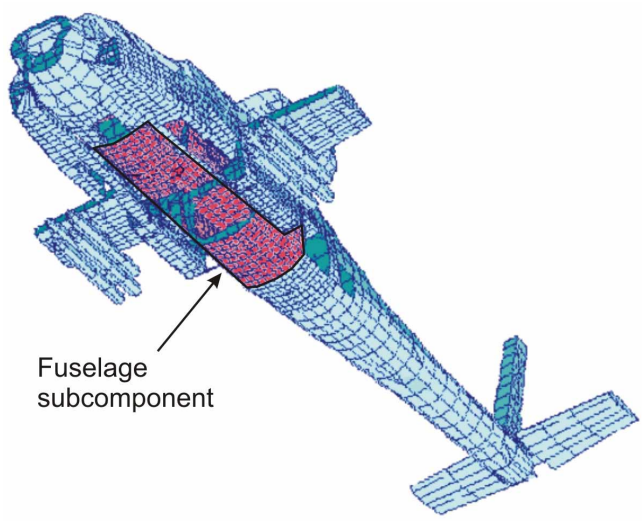

Fig. 10. Apache loads model.

Displacement solutions from the loads model were used to develop interpolated displacement fields, as shown in Fig. 11. The fields are applied as a boundary conditions to the edges of the five-foot model, as shown in Fig. 11b.

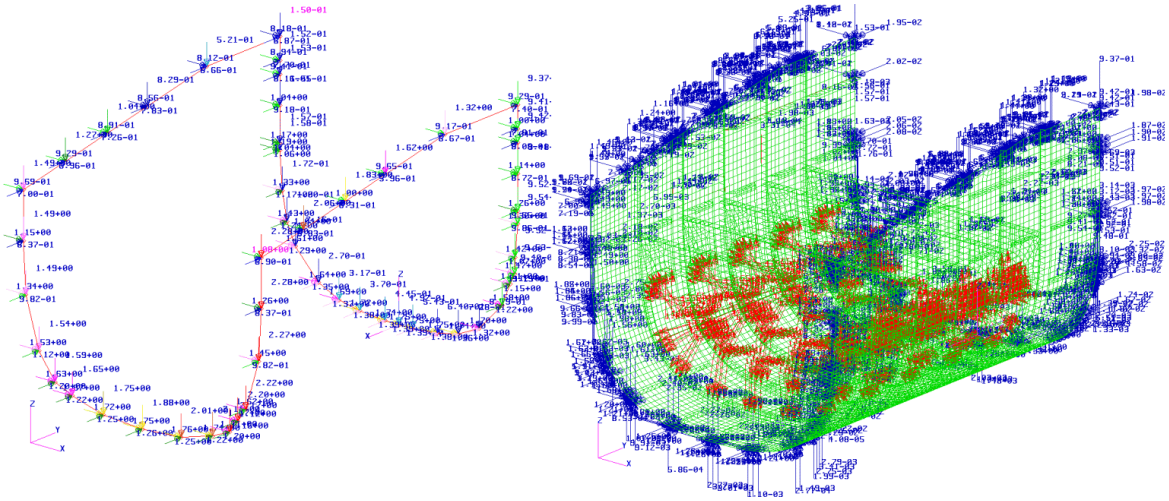

a) Displacement solution from load model

b) Displacement fields as boundary conditions.

Fig. 11. Interpolated displacement fields used as boundary conditions of the five-foot model.

Geometrically nonlinear analyses were performed for the five-foot model under typical Apache flight and transportability conditions. The results of these analyses were displacements, strains, stresses, section forces and moments, and internal forces. These results provide the required information to perform traditional strength and buckling analyses. As examples, deformed plots of the five-foot model for four load cases are shown in Fig. 12.

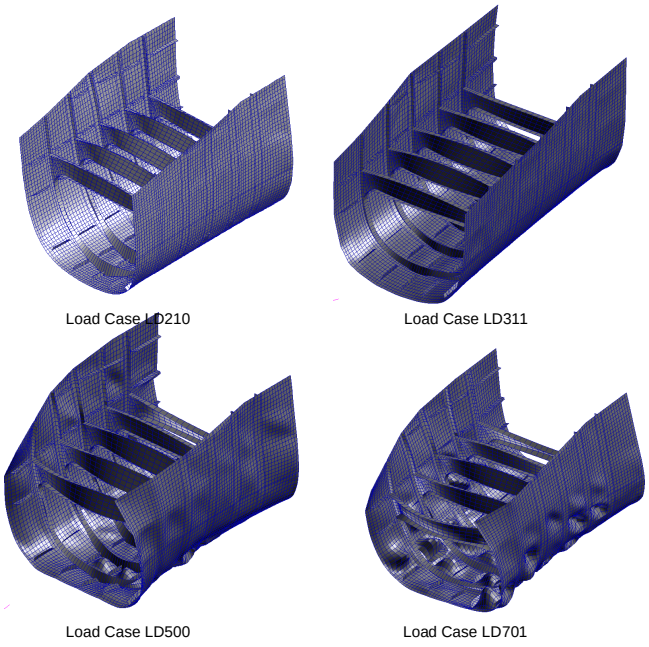

Fig. 12. Deformed plots for four load cases.

The definitions of these load cases are given in Table 2. As shown in Fig. 12, load cases LD210 and LD311 do not exhibit buckling at any of the skin bays. Load cases LD500 and LD701, on the other hand, buckle at several locations and their solution required stabilization through viscous damping.

Table 2. Load Case Definitions

Load Case	Description	Acceleration	Airspeed
LD210	Flight	3.5g	145kt
LD311	Flight	3.5g	164kt
LD500	Transport	N/A	N/A
LD701	Landing	N/A	N/A

Additionally, the delamination failure of the frame to skin joint can be assessed through the distribution of the out-of-plane bending moments. As an example, the out-of-plane bending moment for LD311 is shown in Fig. 13. The maximum out-of-plane frame bending moment (M_x) is at frame 145 closed to the boundary as shown in the figure. However due to boundary effect, the region from stations 125 to 163 and from stringer 4 and below (Fig. 14) are considered valid regions. The out-of-plane bending moment away from the boundary regions, which are shown in Fig. 14, are too low to cause frame pull-off type failure for this flight condition.

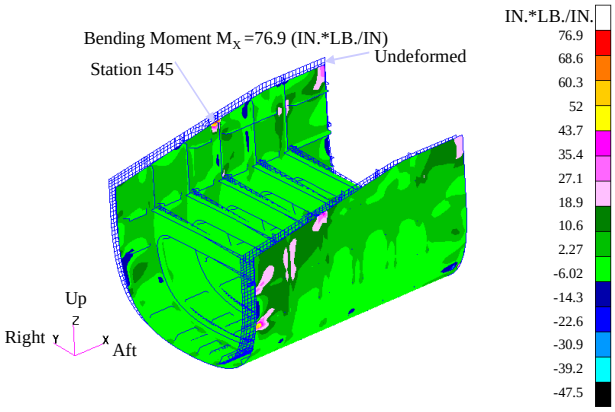

Fig. 13. The out-of-plane bending moment distribution.

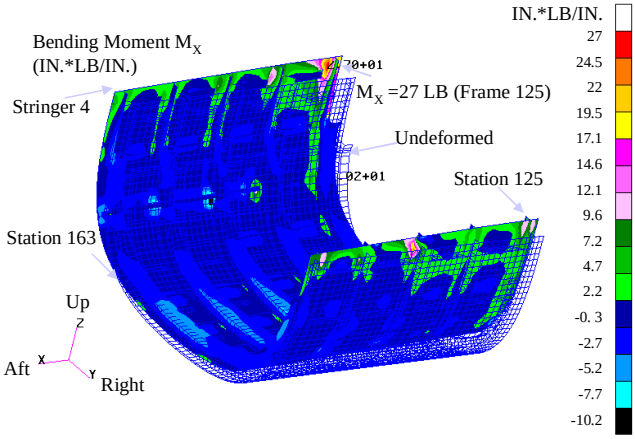

Fig. 14. The out-of-plane bending moment distribution in regions one bay away from the boundaries.

The combination of local and global analyses has created a new analysis methodology, which represents a significant improvement to the state-of-the-art structural strength analysis. This methodology can be used to identify potential failure during the analysis stage, which would have been found out only at the end of a full-scale structural testing by the current state-of-the-art strength analysis. A schematic of the structural analysis processes for a fuselage skin is shown in Fig. 15. The traditional strength analysis starts from the load model to obtain internal loads for skin panels. Each skin panel is analyzed under the internal loads to obtain sizing for that panel. These processes are repeated until satisfactory results are obtained for all the panels. The final sizing is verified by full-scale testing.

The high fidelity methodology adds fracture failure analysis to the strength analyses. Four critical parts form the heart of this methodology. These are representative local coupon testing, local failure analysis, global strength analysis and the crucial link between local analysis and

global analysis. Fig. 15 illustrates how this methodology enhances the current strength analysis processes and identifies potential failures, which would have been found only at the end of a full-scale structural testing.

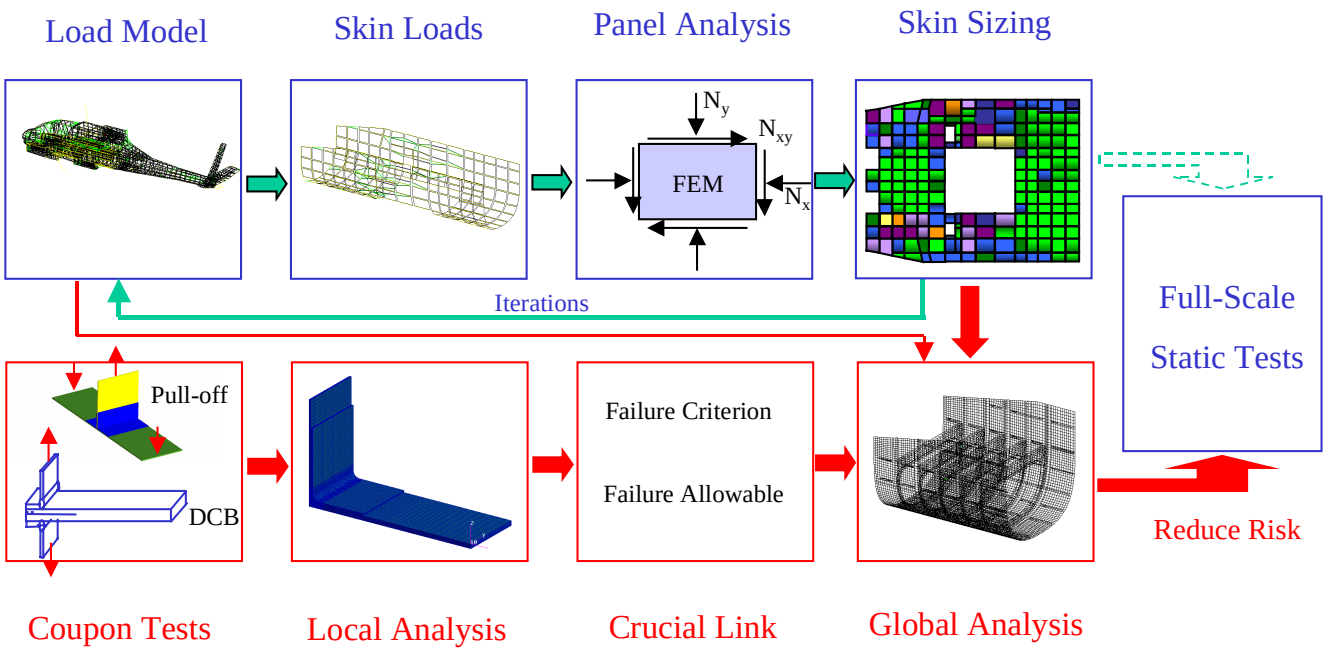

Figure 15. High fidelity delamination failure analysis in the strength analysis processes.

SUMMARY

A high fidelity global/local delamination failure analysis was developed that can be used to validate the design of large composite structures. The methodology is based on four critical components. These components are: i) testing of representative local coupons, ii) local failure analysis, iii) global strength analysis and iv) the crucial link between local analysis and global analysis. The new methodology enhances the current strength analysis processes and identifies potential failures, which may only have been found at the end of a full-scale structural testing by the current state-of-the-art strength analysis. The potential cost saving can be significant. This analysis methodology could help avoid costly failures missed by traditional strength analysis. The analysis methodology is also easy to use because the current FEA already computes the out-of-plane bending moments as a by-product.

REFERENCES

1. "Rotary Wing Structures Technology Demonstration," Cooperative Agreement DAAH-10-98-2-002 with U.S. Army Aviation Applied Technology Directorate, Fort Eustis, Virginia, 1998.
2. Li, J., O'Brien, T. K. and Rousseau, C. Q. "Test and Analysis of Composite Hat Stringer Pull-off Test Specimen," *Journal of the American Helicopter Society*, Vol. 42, No. 4, 1997, pp. 350-357.
3. Li, J., "Flange Delamination Prediction in Composite Structures with Ply Waviness," *AIAA Journal*, Vol. 38, No. 5, May 2000, pp. 893-897.
4. Li, J. "Three-Dimensional Effect in the Prediction of Flange Delamination in Composite Skin-Stringer Pull-off Specimens," Proceedings of American Society for Composites 15th Technical Conference, College Station, Texas, September 25-27, 2000, pp. 983-990.
5. Li, J., Lee, S. M., Lee, E. W., and O'Brien, T. K., " Evaluation of the Edge Crack Torsion (ECT) Test for Mode III Interlaminar Fracture Toughness of Laminated Composites," *Journal of Composites Technology & Research*, JCTRER, Vol. 19, No. 3, 1997, pp. 174-183.
6. Irwin, G. R. 1957. "Analysis of Stresses and Strains near the End of a Crack Traversing a Plate," *Engineering Journal of Applied Mechanics*, Vol. 24, pp. 361-364.
7. Rybicki, E. F. and Kanninen, M. F. 1977. "A Finite Element Calculation of Stress Intensity Factors by a Modified Crack-Closure Integral," *Engineering Fracture Mechanics*, Vol. 9, pp. 931-938.
8. O'Brien, T. K., "Composite Interlaminar Shear Fracture Toughness, G_{IIc}: Shear Measurement or Shear Myth?," *Composite Materials: Fatigue and Fracture, Seventh Volume, ASTM SPT 1330*, 1998, pp. 3-18.